Biointerphases (2012) 7:1
DOI 10.1007/s13758-011-0001-y

IN FOCUS: NANOMEDICINE - ARTICLE

Comparative Stability Studies of Poly(2-methyl-2-oxazoline) and Poly(ethylene glycol) Brush Coatings

Bidhari Pidhatika · Mathias Rodenstein · Yin Chen · Ekaterina Rakhmatullina · Andreas Mühlebach · Canet Acikgöz · Marcus Textor · Rupert Konradi

Received: 19 September 2011 / Accepted: 31 October 2011 / Published online: 9 February 2012

Abstract Non-fouling surfaces that resist non-specific adsorption of proteins, bacteria, and higher organisms are of particular interest in diverse applications ranging from marine coatings to diagnostic devices and biomedical implants. Poly(ethylene glycol) (PEG) is the most frequently used polymer to impart surfaces with such non-fouling properties. Nevertheless, limitations in PEG stability have stimulated research on alternative polymers that are potentially more stable than PEG. Among them, we previously investigated poly(2-methyl-2-oxazoline) (PMOXA), a peptidomimetic polymer, and found that PMOXA shows excellent anti-fouling properties. Here, we compare the stability of films self-assembled from graft copolymers exposing a dense brush layer of PEG and PMOXA side chains, respectively, in physiological and oxidative media. Before media exposure both film types prevented the adsorption of full serum proteins to below the detection limit of optical waveguide in situ measurements. Before and after media exposure for up to 2 weeks, the total film thickness, chemical composition, and total adsorbed mass of the films were quantified using variable angle spectroscopic ellipsometry (VASE), X-ray photoelectron spectroscopy (XPS), and optical waveguide lightmode spectroscopy (OWLS), respectively. We found (i) that PMOXA graft copolymer films were significantly more stable than PEG graft copolymer films and kept their protein-repellent properties under all investigated conditions and (ii) that film degradation was due to side chain degradation rather than due to copolymer desorption.

Andreas Mühlebach: Andreas Mühlebach, his wife Claudine and daughter Simone, lost their lives in a tragic accident in the Swiss mountains on 6 July 2010. In the context of a long-term collaboration with ETH Zurich, Andreas made substantial contributions to both this specific publication and the development of new polymers for the biomaterials field in general. We deeply miss him as an outstanding, dedicated scientist, colleague, and friend.

This article is part of the Topical Collection "In Focus: Nanomedicine".

B. Pidhatika (✉) · M. Rodenstein · Y. Chen · E. Rakhmatullina · C. Acikgöz · M. Textor · R. Konradi
Laboratory for Surface Science and Technology, Department of Materials, ETH Zurich, Wolfgang-Pauli-Strasse 10, 8093 Zurich, Switzerland
e-mail: bidhari.pidhatika@alumni.ethz.ch

B. Pidhatika
Department of (Polymer) Materials, Academy of Leather Technology, Ministry of Industry, Republic of Indonesia, Jl. Ringroad Selatan, Ds. Glugo, Panggungharjo, Sewon, Bantul, Yogyakarta, Indonesia

Y. Chen
Bioengineering Program, The Hong Kong University of Science and Technology, Clear Water Bay, Kowloon, Hong Kong SAR

E. Rakhmatullina
Department of Preventive, Restorative and Pediatric Dentistry, University of Bern, Freiburgstrasse 7, 3010 Bern, Switzerland

A. Mühlebach
BASF Switzerland, 4002 Basel, Switzerland

R. Konradi
BASF SE, Polymer Research, 67056 Ludwigshafen, Germany

1 Introduction

Densely-grafted polymer films (brush regime) on metal oxide surfaces are frequently applied to convey biopassive properties, i.e. to reduce protein adsorption [1], bacteria adhesion [2], and cell-surface interactions [3]. Poly(ethylene glycol) (PEG) [4] represents the gold standard in this respect [2, 5–15], but other polymers such as polyacrylamide (PAAM) [16], poly(N-vinyl pyrrolidone) (PVP) [17], and peptidomimetic polymers (PMP1 [18]) as well as poly(2-methyl-2-oxazoline) (PMOXA) [19–21] have been shown to be similarly effective.

The preference for PEG-based non-fouling materials is due to its biocompatibility, non-immunogenic and non-cytotoxic properties [22]. Moreover, PEG has been approved by the US food and drug administration (FDA) for application in pharmaceutical and coating technologies [22–24]. Nevertheless, several limitations of PEG-based technology have been reported. One of them is loss of biopassive function in case of long-term application [3, 25–27]. McGary [28] reported PEG degradation upon aging in aqueous solutions. It was believed that PEG degrades by auto-oxidation due to repetitive oxygen units in its structure. Moreover, it has been reported that PEG degrades autocatalytically in bulk (solid state) [29] as well as in surface-bound state [30–33] and in dilute solutions [25]. A discussion of complications associated with the non-biodegradability and tendency to autoxidation in the presence of oxygen can also be found in a recent review by Knop et al. [34].

Zoulalian et al. [35] reported instability of PEG-based films on titanium oxide (TiO_2) and niobium oxide (Nb_2O_5) upon exposure to different aqueous media, with and without exposure to light. The authors proposed that photocatalytic activity of certain substrates (such as TiO_2, but not Nb_2O_5) is one of the factors affecting PEG (and possibly other polymer) degradation. Moreover, the authors suggested that 4-(2-hydroxyethyl) piperazine-1-ethanesulfonic acid (HEPES) contributes to degradation of PEG. Wet oxidation of PEG with various molecular weights between 2 and 20 kDa under high pressure and at elevated temperature was investigated by Imamura et al. [36]. The authors suggested that PEG susceptibility to degradation correlated to the ease of intramolecular hydrogen abstraction in the propagation step of oxidation.

Polypeptides or peptidomimetic polymers are potential alternatives to PEG for applications where non-fouling properties are required. For example, Chilkoti et al. [37] reported the application of artificial thermoresponsive elastin-like polypeptides in drug delivery to combat solid tumours in mice. It was found that this peptidomimetic polymer enhanced drug accumulation by ~5-fold at the tumour site level if compared to that delivered using PEG [38]. This finding provides evidence that the peptidomimetic polymer created a stable, stealth drug carrier upon exposure to serum protein and blood cells contained in blood plasma of the mice. Also, Messersmith [18] performed a long-term study in cell culture medium using a mono(ethylene glycol)-functionalized peptidomimetic polymer as surface coating on titania surfaces, anchored through an oligo(DOPA-lysine) binding moiety. The authors reported resistance to cell adhesion for more than 5 months, which is much longer than what can be achieved with PEG-based systems. However, it remains unclear to what extent the ethylene glycol functionalization is essential to long-term performance of this particular peptidomimetic polymer.

Another promising polymer with a peptidomimetic structure is poly(2-methyl-2-oxazoline) (PMOXA) [19–21, 39]. PMOXA has been reported to have favourable properties for a number of biological and medical applications, such as stealth liposomes for cell targeting and drug delivery [40–45]. Protein adsorption [19] and bacteria adhesion [20] on PMOXA films have already been compared to those on PEG films, where PMOXA has shown comparable non-fouling properties as PEG if organized as a brush with optimum density. However, no systematic comparative stability study between PMOXA and PEG has so far been published to the best of our knowledge.

In this study, the stability of PMOXA films was compared to that of PEG films with Nb_2O_5 as substrate. The chemical structure of PMOXA suggests that this polymer is less prone to oxidation compared to PEG since ***N***-vicinal C–H bonds are less polarized than ***O***-vicinal C–H bonds. Thus degradation initiated through hydrogen abstraction in the PMOXA chains is presumably less likely. To perform a direct comparison, the PMOXA-based surface coating was designed in analogy to PEG-based coating in previously reported quantitative study [9], i.e. PLL-X graft copolymers (X = PMOXA or PEG). These graft copolymers present a polycationic poly(L-lysine) backbone that allows spontaneous assembly and anchoring of the grafted copolymer to negatively charged surfaces. Nb_2O_5 is a particularly suitable substrate considering its high negative surface charge density [1].

Polymer composition, film thickness and surface densities are considered potential factors that affect stability of polymer films. Therefore, PLL-PEG and PLL-PMOXA films with controlled film thicknesses and surface densities were chosen for the comparative stability studies. Water, salts, pH, and oxidative substances are important aspects with regard to the stability of polymeric surfaces in biomaterial applications [46–48]. In this study, the PLL-PMOXA and PLL-PEG films were therefore exposed to the following stability test solutions:

1. A solution of 10 mM H_2O_2. H_2O_2 was used to represent oxidative substances secreted by cells such as macrophages or bacteria.

2. A solution of 160 mM ion concentration that mimics the ionic strength of body fluid. The solution contained 10 mM HEPES + 150 mM NaCl. The 150 mM NaCl presents a solution of salt that is isotonic with the body fluids, while the 10 mM HEPES acts as a buffering agent to maintain the physiological pH ($\sim$7.4).
3. A solution of 10 mM H_2O_2 + 10 mM HEPES + 150 mM NaCl. This solution mimics the physiological solution (10 mM HEPES + 150 mM NaCl), in the presence of an oxidative substance (10 mM H_2O_2).

The film stability was investigated using three different surface characterization techniques, i.e. variable angle spectroscopic ellipsometry (VASE), X-ray photoelectron spectroscopy (XPS) and optical waveguide lightmode spectroscopy (OWLS). VASE allows for a fast and sensitive determination of total film thickness. XPS provides chemical information of the studied surfaces. OWLS was used to monitor in situ the degradation kinetics in real time. The non-fouling properties of the copolymer films before and after stability test were evaluated from protein (human serum) resistance test.

2 Experimental

2.1 Water and Chemical Products

2.1.1 PLL, PLL-PEG, and PLL-PMOXA

PLL was purchased from Sigma-Aldrich. PLL-PEG polymers were purchased from Surface Solutions AG (Zurich, Switzerland). PLL-PMOXA polymers were synthesized and characterized using matrix-assisted laser desorption/ionization-time of flight (MALDI-ToF) and proton nuclear magnetic resonance spectroscopy (^{1}H NMR) following the previously published protocol [21, 39].

2.1.2 Water

All stability test solutions were prepared by using ultrapure water. Ultrapure water was produced in a Milli-Q system Gradient A 10 from Millipore (Zug, Switzerland). The system is equipped with Elix3 that removes 95–99% of inorganic ions, 99% of dissolved organic compounds, bacteria, and particulates.

2.1.3 H_2O_2, NaCl, and HEPES

Hydrogen peroxide 30% H_2O_2 (perhydrol*) pro analysis (p.a) was purchased from Merck KGaA (Damstadt, Germany). It contains impurities such as $\leq$40 ppm free acid as H_2SO_4, $\leq$50 ppm nonvolatile matter, and diverse metal impurities such as Al, Ca, Na, etc., in which each of them present in a concentration of <0.5 ppm. NaCl was purchased from Sigma-Aldrich. HEPES (4-(2-hydroxyethyl)-1-piperazine ethane sulfonic acid) and other chemicals used for the preparation of physiological solution were purchased from Fluka (Buchs, Switzerland).

2.1.4 Human Serum Proteins

Human serum proteins (Precinorm U) were purchased from Roche Diagnostics GmbH (Mannheim, Germany). The lyophilized powder was dissolved in ultrapure water as recommended by the supplier. The solution contains human serum components, along with enzymes and other additives, with a total concentration of approximately 70 mg/ml, which is about equal to that found in clinically normal human serum. The solution was divided into 0.5 ml aliquots in eppendorfs and stored in a -20°C freezer. The serum solution was defrosted at room temperature prior to use.

2.2 Stability Test Solutions

All stability test solutions were freshly prepared before the stability test.

2.2.1 A Solution of 10 mM H_2O_2

10 mM H_2O_2 solution was prepared by dilution of the commercially available hydrogen peroxide 30% H_2O_2 (perhydrol*) pro analysis (p.a) from Merck KGaA in ultrapure water. The pH of the solution was approximately 7 as measured with pH paper.

2.2.2 A Solution of 160 mM Ion Concentration (10 mM HEPES + 150 mM NaCl)

10 mM HEPES solution with additional 150 mM NaCl was prepared by dissolving the commercially available HEPES from Fluka and NaCl from Sigma-Aldrich in ultrapure water. The pH of the solution was then measured using pH-meter and adjusted to pH 7.4 by addition of 6 M NaOH. This solution is also called HEPES2 buffer.

2.2.3 A Physiological Solution in the Presence of Oxidative Substance (10 mM H_2O_2 + 10 mM HEPES + 150 mM NaCl)

The solution was prepared by dilution of the commercially available hydrogen peroxide 30% H_2O_2 (perhydrol*) pro analysis (p.a) from Merck KGaA in the solution of 10 mM HEPES + 150 mM NaCl described above.

2.3 Substrate and Surface Modification Protocol

2.3.1 Substrate

The silicon wafers for VASE and XPS investigations were purchased from Si-Mat Silicon Materials (Landsberg, Germany). The silicon wafers were sputter-coated with a 21-nm-thick Nb_2O_5 layer (reactive magnetron sputtering, Paul Scherrer Institute, Villigen, Switzerland). The waveguides (OW2400) for OWLS experiments were purchased from Microvacuum Ltd. (Budapest, Hungary). Each waveguide consists of a 0.5-mm-thick AF45 glass substrate and a 200-nm-thick $Si_{0.75}Ti_{0.25}O_2$ waveguiding layer on the surface. An additional 6-nm-thick Nb_2O_5 layer was sputter-coated on the top of the waveguiding layer.

2.3.2 Surface Modification

Prior to the copolymer adsorption, Nb_2O_5 substrates were ultrasonicated for 2 × 10 min in toluene (Fluka) followed by 2 × 10 min of ultrasonication in 2-propanol (Fluka) and blow-drying under a stream of nitrogen. Nb_2O_5 substrates were subsequently cleaned by oxygen plasma treatment for 2 min (Plasma cleaner/sterilizer PDC-32G, Harrick scientific products Inc.).

Polymer films were prepared by dip and rinse protocol [20]. Briefly, for *ex situ* experiments using VASE and XPS techniques, the polymers were dissolved at 0.1 mg/ml concentration in a filtered (0.22 μm) HEPES buffer solution containing 10 mM HEPES supplemented with 150 mM NaCl and adjusted to pH 7.4 (HEPES2). Then, 50 μl of copolymer solutions were placed onto the freshly pre-cleaned substrates completely covering their surfaces. Polymer adsorption was allowed to proceed for around 2 h, followed by extensive washing with ultrapure water and blow-drying under a stream of nitrogen. The surface modification protocol for in situ experiments using OWLS techniques is described below.

2.4 Stability Test Protocol

Stability of the (ex situ) prepared films was tested by immersion in different stability test solutions at room temperature in γ-sterilized polystyrene cell-plate boxes (TPP, test plates, 92024). To protect the samples from daylight, the cell-plate boxes were wrapped with a piece of aluminum foil. The immersion time was varied between 5 h and 2 weeks. Sterile condition during stability experiments was assured by filtering all solutions before use with a 0.22 μm filter. Moreover, the preparation of copolymer films and the stability tests were performed in a sterile flow box.

At the end of stability test, the samples were rinsed with ultrapure water and dried under nitrogen stream prior to their characterizations of thickness (VASE) and surface composition (XPS) for the detection of polymer degradation. The copolymer films were subsequently re-hydrated by placing ultrapure water on top of the samples, fully covering the surface, for 30 min. The non-fouling properties of the copolymer films after stability tests were then evaluated by exposing the films to human serum solution for 15 min, followed by rinsing with ultrapure water, and drying under nitrogen stream. The change of film thickness after exposure to serum proteins was measured by VASE. The stability test protocol for in situ experiments using OWLS technique is described below.

2.5 Characterization Techniques

2.5.1 VASE

The dry copolymer film thickness was measured in air by variable angle spectroscopic ellipsometry (VASE) using the M-2000F variable angle spectroscopic ellipsometer (J. A. Woollam Co., Inc.). The measurements were performed at 65°, 70° and 75° relative to the surface normal, under ambient conditions and in the spectral range of 370–1,000 nm. Ellipsometry data were fitted with a multilayer model using the custom analysis software (WVASE 32) and a Cauchy model ($A_n = 1.45$, $B_n = 0.01$, $C_n = 0$) [49, 50] to obtain the dry thickness of the adsorbed polymer layers.

2.5.2 XPS

A Sigma2 instrument (Thermo Fisher Scientific, Loughborough, Great Britain) was utilized for routine XPS experiments in this study. The Sigma2 is equipped with a UHV chamber (pressure $<10^{-6}$ Pa during measurements) and an Al-Kα non-monochromated X-ray source (300 W, $hv = 1486.6$ eV) illuminating the sample at an angle of 54° to the surface normal. A hemispherical analyzer is mounted at 0° with respect to the surface normal, thus operating at the magic source-analyzer angle, which eliminates the need for angular-distribution correction.

The spot size of the analyzed area (large-area mode) was 400 μm, and the results therefore represented a laterally averaged chemical composition. Standard measurements comprised averages over nine (for C, and N) or three (for Nb and O) scans for each element with pass energies of 25 eV, as well as survey scans with pass energy of 50 eV. The dwell time was left at 100 ms at all times, resulting in 3–5 min measurement time per spot for each element, accumulating to about 30 min for a complete elemental scan on each measuring position.

2.5.3 OWLS

OWLS measurements were performed on an OWLS 110 with BioSense 2.2 software from Microvacuum Ltd. (Budapest, Hungary). OWLS allows for quantitative in situ monitoring of copolymer and serum adsorption in a flow-through cell (typical cell dimension: $8 \times 2 \times 1$ mm^3 or 16 µl-volume). OWLS experiments were performed following previously described procedure [19, 20], i.e. by sequential injections of solutions.

Incubation of the Nb_2O_5-coated waveguides in copolymer solutions for 30–120 min resulted in the formation of a saturated layer. Subsequently, a stability test solution was injected followed by further 5 h incubation. Incubation of the (degraded) films in full human serum for 15 min followed by rinsing allowed determination of the adsorbed protein mass. The experiments were repeated three times for each copolymer.

3 Results and Discussion

3.1 Polymer Films

PLL, PLL-PEG and PLL-PMOXA polymers were immobilized onto Nb_2O_5 surfaces via electrostatic interaction between the negatively charged substrate and positively charged free lysine residues of the PLL-backbone [19, 20]. Both copolymer systems have identical PLL backbones (20 kDa as HBr salts, with approximately 96 lysine repeating units).

Side chain molecular weights were chosen for the purpose of comparing PMOXA and PEG polymer having approximately the same monomer repeating units (polymerization degree). PMOXA 4 kDa with approximately 44 MOXA-mers per PMOXA chain is comparable to PEG 2 kDa with approximately 50 EG-mers per PEG chain. Similarly, PMOXA 8 kDa (approximately 90 MOXA-mers per PMOXA chain) is comparable to PEG 5 kDa (approximately 113 EG-mers per PEG chain).

Grafting density (α) was defined as the number of side PEG or PMOXA chains per number of lysine units (PMOXA/lysine or PEG/lysine). PLL-PMOXA and PLL-PEG copolymers having similar grafting density of around 0.3 were studied. The similar grafting density grants equal amount of free NH_3^+ anchoring groups for the attachment to Nb_2O_5 and thus equal adhesion strength. Figure 1 shows the chemical structures of the two copolymers immobilized on Nb_2O_5.

The copolymers used in this study were PLL-PMOXA$_4$ ($\alpha = 0.33$), PLL-PMOXA$_8$ ($\alpha = 0.25$), PLL-PEG$_2$ ($\alpha = 0.31$) and PLL-PEG$_5$ ($\alpha = 0.28$), with the following notation: PLL-PEG$_5$ ($\alpha = 0.28$) refers to PEG with molecular weight of 5 kDa, grafted to PLL with molecular weight of 20 kDa (as HBr salt), and a PEG grafting density of 0.28 PEG/lysine and correspondingly for the other copolymers.

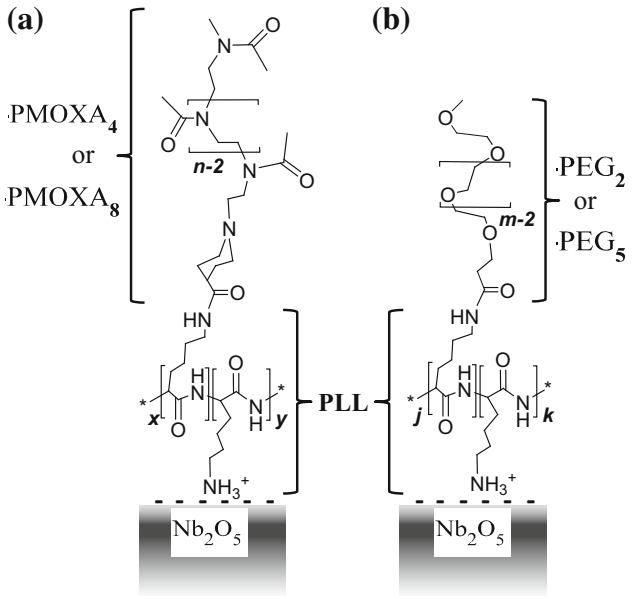

Fig. 1 Scheme of the two copolymers adsorbed on Nb_2O_5 surfaces: **a** PLL-PMOXA with ***n*** number of 2-methyl-2-oxazoline (MOXA) repeating units, grafting density $\alpha = x/(x + y)$ and **b** PLL-PEG with ***m*** number of ethylene glycol (EG) repeating units, grafting density $\alpha = j/(j + k)$. The number following the polymer abbreviation (PMOXA, PEG) indicates the molecular weight in kDa

3.2 Characterization of the Initial Polymer Films

The copolymer film thickness and mass were analyzed using VASE and OWLS, respectively. Surface densities of macromolecules, side chains as well as monomer units could be calculated from combined OWLS and ^{1}H NMR analysis following previously published equations [9] and are presented in Table 1. PLL-PEG$_5$ showed comparable dry thickness and adsorbed mass as PLL-PMOXA$_8$ (Table 1, entries 2 and 3). The former also showed similarities with PLL-PMOXA$_4$ in terms of molecular and side chain surface densities (Table 1, entries 4 and 5). PLL-PEG$_2$ had nearly identical monomer surface density as both PLL-PMOXA$_4$ and PLL-PMOXA$_8$ (Table 1, entry 6).

The adsorbed polymer mass for PLL-PEG$_2$ is somewhat lower due to the lower side-chain molecular weight. The maximum in adsorbed copolymer mass for each system is typically reached at a medium grafting density where an almost defect-free monolayer is formed on the surface. This maximum corresponds to a minimum in protein adsorption and is a result of the interplay of increasing side chain density and accordingly adsorbed mass at low to medium grafting densities and an increasingly weak

Table 1 Characteristics of the four copolymers and the films after surface assembly: molecular weights, film thicknesses, adsorbed masses, surface densities of molecules, side chains, and monomers

Entry no.	Analyzed parameter	PLL-PMOXA$_4$ ($\alpha = 0.33$)	PLL-PMOXA$_8$ ($\alpha = 0.25$)	PLL-PEG$_2$ ($\alpha = 0.31$)	PLL-PEG$_5$ ($\alpha = 0.28$)	Nb_2O_5
1	Molecular weight of polymer (kDa)	140	204	72	145	n/a
2	Polymer thickness (nm)	2.07 ± 0.17	2.36 ± 0.04	1.30 ± 0.03	2.47 ± 0.10	n/a
3	Polymer mass on the surface (ng/cm^2)	210 ± 10	240 ± 28	152 ± 16	245 ± 75	n/a
4	Molecular surface density ($\times 10^{-3}$ nm^{-2}),	8.7 ± 0.9	7.1 ± 0.8	12.7 ± 1.3	10.2 ± 3.2	n/a
5	Side chain surface density (nm^{-2})	0.28 ± 0.01	0.17 ± 0.02	0.39 ± 0.05	0.27 ± 0.09	n/a
6	Monomer surface density (nm^{-2})	14 ± 1	16 ± 2	18 ± 2	31 ± 10	n/a
7	Serum thickness on initial polymer layer (nm)	0.03 ± 0.03	0.02 ± 0.03	0.02 ± 0.01	0.01 ± 0.01	6.4 ± 0.3
8	Serum mass on initial polymer layer (ng/cm^2)	1 ± 2	0 ± 1	2 ± 3	0 ± 1	223 ± 22

Furthermore, data related to the degree of serum protein adsorption on the polymeric surfaces and Nb_2O_5 bare substrate: adsorbed serum thicknesses and masses

binding to the surface due to increasing steric repulsion of the bottle brushes from the surface and decreasing backbone charge density with increasing grafting density at high grafting densities. These effects have been discussed in detail in earlier studies [9, 19].

Before exposure to stability test solution, all PLL-PMOXA and PLL-PEG copolymers resisted serum (Table 1, entries 7 and 8). Serum protein adsorption on the unprotected Nb_2O_5 and PLL interfaces was found to be in a good agreement with previously reported results [1].

Typical XPS spectra from each freshly prepared copolymer film on Nb_2O_5 surface are exemplarily presented in Table 2. For each film, at least three spectra were acquired from three different positions on the surface. The spectra were then quantitatively evaluated to obtain atomic percentages (atomic-%), and the values are presented in Table 3. In general, the experimental values (calculated from the acquired spectra) were in good agreement with the theoretical ones (calculated based on composition stoichiometry). PLL-PEG$_2$ shows a too high experimental value of **O**=C atomic-% compared to the theoretical one. This might be attributed to the presence of hydroxyl groups as the NH_3^+ counterions on the surface. Furthermore, PLL-PEG$_2$ and PLL-PEG$_5$ show too low experimental values of **N**H_3^+ atomic-% compared to the theoretical ones. This phenomenon might be due to neutralization of NH_3^+ by OH^- or Br^- in the dry state. The binding energy for each binding state (Table 3) was in agreement with literature [51]. Furthermore, Carbon (C1s) to niobium (Nb3d) ratio of signal intensities (C/Nb) and Nitrogen (N1s) to Nb3d ratio (N/Nb) of the initial films were evaluated and presented in Table 4 (entries 1 and 2). These initial values of freshly prepared films are used in the next section for the evaluation of C/Nb and N/Nb remaining ratios of the films after stability tests.

3.3 Stability Study

3.3.1 Stability upon Exposure to 10 mM H_2O_2

Copolymer-modified surfaces were immersed in 10 mM H_2O_2 solution and were analyzed after different periods from 5 h up to 336 h. Figure 2a shows the remaining copolymer thickness while Fig. 2b and c show serum thickness. Both parameters, remaining copolymer thickness and serum thickness, were plotted as a function of the incubation time of the copolymer films in stability test solutions. The degradation rate was observed to be significantly slower for both types of PLL-PMOXA compared to PLL-PEG films (Fig. 2a). More than 80% of PLL-PMOXA$_4$ and PLL-PMOXA$_8$ thickness remained after 336 h, which was twice the remaining thickness of PLL-PEG$_2$ and PLL-PEG$_5$.

For both types of copolymers, a correlation between degradation of copolymer films and their biopassive function was observed, i.e. serum thickness increased with time (or as the copolymer thickness decreased) (Fig. 2b, c). A high adsorbed serum thickness ($\sim$3.5 nm) on PLL-PEG$_2$ film was detected when the remaining thickness of the polymeric layer was about 60% (compare Fig. 2a, b, at 168 h). At the same copolymer remaining thickness ($\sim$60%), however, PLL-PEG$_5$ still showed a low adsorbed serum thickness of $\sim$0.2 nm (Fig. 2c). The degradation kinetics of PLL-PEG$_2$ and PLL-PEG$_5$ as judged from the relative thickness reduction (Fig. 2a) were similar; however the PLL-PEG$_5$ film had a significantly higher initial EG monomer surface density (Table 1, entry 6). Therefore, for the same remaining thickness of 60%, significantly less serum proteins were adsorbed on the PLL-PEG$_5$ compared to the PLL-PEG$_2$ film. For PLL-PMOXA$_4$ and PLL-PMOXA$_8$, no significant difference in film degradation rate

Table 2 The assignment of component-resolved XPS spectra for bare Nb_2O_5, and Nb_2O_5 coated with PLL-PEG_5 ($\alpha = 0.28$) and PLL-$PMOXA_4$ ($\alpha = 0.33$)

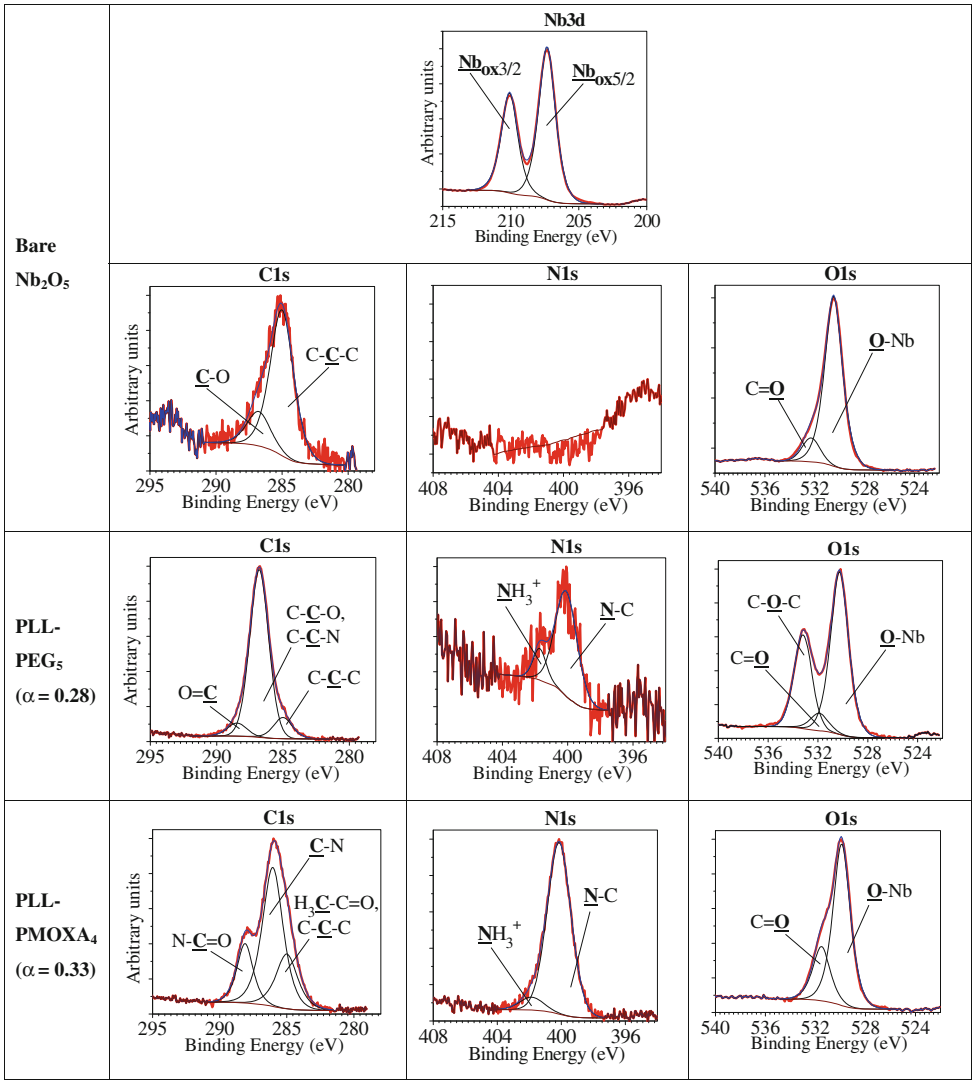

was observed (Fig. 2a), and only slight difference was observed in serum adsorption where PLL-$PMOXA_4$ showed slightly higher values (Fig. 2c). This phenomenon is probably a consequence of the initial monomer surface density of PLL-$PMOXA_4$ being slightly lower than that of PLL-$PMOXA_8$ (Table 1, entry 6).

The C1s/Nb3d (C/Nb) and N1s/Nb3d (N/Nb) ratios after stability test are presented in Fig. 3. The total C/Nb and N/Nb ratios measured for PLL-PMOXA copolymer films did not significantly decrease after 1 day and 1 week (only ~5% decrease), indicating their stability upon exposure to 10 mM H_2O_2 (Fig. 3a). Degradation of PLL-PEG films proceeded comparatively faster as the C/Nb ratio reduced by ~20% upon 1 week incubation (Fig. 3b). On the other hand, the N/Nb ratio was found to be more stable (only ~5% reduction after 1 week). Because N1 s is specific to PLL for a PLL-PEG film, the difference between C/Nb and N/Nb indicates that the PEG chains degraded preferentially to PLL. The slight reduction in N/Nb for PLL-$PMOXA_8$, PLL-PEG_2 and PLL-PEG_5 as compared to PLL-$PMOXA_4$ is hardly statistically significant. It might stem from a different degradation route involving the desorption of entire copolymer molecules. This might be triggered through either a first degradation of the side chains or by an initial non-perfect monolayer conformation. The stability of PLL was evident from a control stability experiment on a PLL film for which the N/Nb ratio reduced by only ~5% after 1 week exposure to 10 mM H_2O_2 (data not shown).

Table 3 XPS data for bare Nb_2O_5, and Nb_2O_5 coated with PLL-PEG_2 ($\alpha = 0.31$), PLL-PEG_5 ($\alpha = 0.28$), PLL-$PMOXA_4$ ($\alpha = 0.33$), and PLL-$PMOXA_8$ ($\alpha = 0.28$): element orbital, the assignment of components with their binding state, binding energy, and theoretical and experimental composition (in atomic percentages)

Element orbital	Binding state	Binding energy (eV)	Atomic-%	
			Theoretical	Experimental
Bare Nb_2O_5				
O1s	$\underline{\mathbf{O}}_{ox}$	530.5	71.0	68.6 ± 1.1
Nb3d	$\underline{\mathbf{Nb}}_{ox\ 5/2}$	207.3	29.0	32.2 ± 0.1
	$\underline{\mathbf{Nb}}_{ox\ 3/2}$	210.1		
PLL-PEG_2 ($\alpha = 0.31$)				
C1s	C–**C**–C	285.0	7.1	8.3 ± 0.5
	C–**C**–O and C–**C**–N	286.7	57.1	51.9 ± 0.9
	C=O	288.5	2.3	2.8 ± 0.4
O1s	**O**=C	531.8	2.3	9.5 ± 0.4[a]
	C–**O**–C	533.1	27.7	24.1 ± 0.8
N1s	**N**–C	400.1	2.3	2.5 ± 0.1
	$\underline{\mathbf{N}}H_3^+$	401.8	1.2	0.8 ± 0.1
PLL-PEG_5 ($\alpha = 0.28$)				
C1s	C–**C**–C	285.0	4.1	5.4 ± 0.5
	C–**C**–O and C–**C**–N	286.7	59.0	55.8 ± 1.3
	C=O	288.6	1.3	2.1 ± 0.2
O1s	**O**=C	531.8	1.3	6.3 ± 1.3[a]
	C–**O**–C	533.1	32.2	28.5 ± 0.7
N1s	**N**–C	400.1	1.3	1.6 ± 0.1
	$\underline{\mathbf{N}}H_3^+$	401.8	0.7	0.2 ± 0.2[b]
PLL-$PMOXA_4$ ($\alpha = 0.33$)				
C1s	H_3**C**–C=O and C–**C**–C	285.0	19.4	14.7 ± 0.3
	C–N	286.1	31.3	36.1 ± 0.3
	N–**C**=O	288.2	16.1	13.4 ± 0.3
O1s	**O**=C	531.7	16.1	19.1 ± 0.4
N1s	**N**–C	400.2	16.4	15.5 ± 0.2
	$\underline{\mathbf{N}}H_3^+$	401.9	0.6	1.0 ± 0.2
PLL-$PMOXA_8$ ($\alpha = 0.25$)				
C1s	H_3**C**–C=O and C–**C**–C	285.0	18.1	16.2 ± 0.4
	C–N	286.1	32.3	34.3 ± 1.2
	N–**C**=O	288.1	16.4	13.3 ± 0.4
O1s	**O**=C	531.6	16.4	19.3 ± 1.5
N1s	**N**–C	400.2	16.5	15.8 ± 0.4
	$\underline{\mathbf{N}}H_3^+$	402.0	0.4	1.0 ± 0.1

[a] Too high **O**=C value might come from hydroxyl groups (as NH_3^+ counterions) on the surface

[b] Too low $\underline{\mathbf{N}}H_3^+$ value might be due to neutralization of NH_3^+ by OH^- or Br^- in dry state

Table 4 Characteristics of the four copolymers and the films after surface assembly: C/Nb and N/Nb ratios before stability tests, evaluated from XPS analysis

Entry no.	Analyzed parameter	PLL-$PMOXA_4$ ($\alpha = 0.33$)	PLL-$PMOXA_8$ ($\alpha = 0.25$)	PLL-PEG_2 ($\alpha = 0.31$)	PLL-PEG_5 ($\alpha = 0.28$)	Nb_2O_5
1	C/Nb	1.87 ± 0.06	2.26 ± 0.05	1.32 ± 0.07	2.22 ± 0.08	0.22 ± 0.01
2	N/Nb	0.49 ± 0.03	0.60 ± 0.01	0.07 ± 0.00	0.06 ± 0.01	n/a

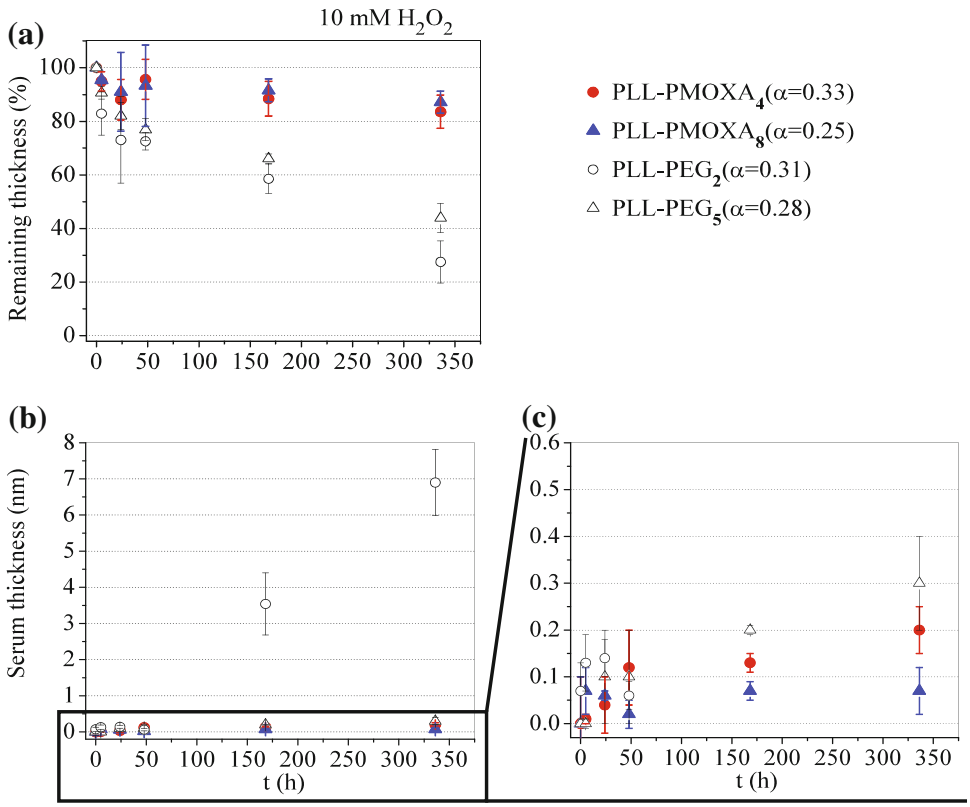

Fig. 2 **a** Remaining thickness of polymer films after stability test in 10 mM H_2O_2, and **b**, **c** corresponding adsorbed serum thickness

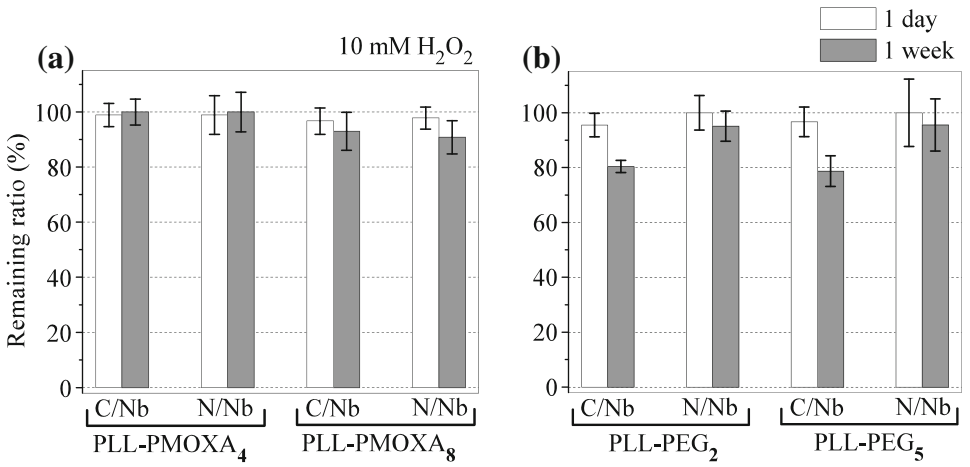

Fig. 3 Remaining C/Nb and N/Nb after 1 day and 1 week stability tests in 10 mM H_2O_2 for **a** PLL-PMOXA and **b** PLL-PEG films. Values were normalized to the initial values of the respective film

3.3.2 Stability upon Exposure to 160 mM Ion Concentration (10 mM HEPES + 150 mM NaCl, pH = 7.4)

A solution of 160 mM ion concentration containing 10 mM HEPES + 150 mM NaCl was used to mimic the physiological solution. Copolymer films were exposed to this solution for the same duration as applied in the experiments with 10 mM H_2O_2 solution.

All PLL-PEG and PLL-PMOXA films degraded upon incubation in physiological solution but to a different extent, with PLL-PMOXA exhibiting higher stability (Fig. 4a). Polymer thickness decreased and remaining biopassive properties correlated well as evident from the serum adsorbed mass data (Fig. 4b, c). Figure 4a shows similar film degradation rate of PLL-PEG$_2$ and PLL-PEG$_5$. However, Fig. 4b shows significant difference in serum thickness on PLL-PEG$_2$ and PLL-PEG$_5$. This is due to the higher initial monomer surface density of PLL-PEG$_5$ compared to PLL-PEG$_2$ (Table 1, entry 6). For PLL-PMOXA$_4$ and PLL-PMOXA$_8$ films, Fig. 4a shows similar film degradation rate, while Fig. 4c shows 0.1–0.2 nm difference in serum thickness as a function of time, with PLL-PMOXA$_8$ showing higher values. This difference

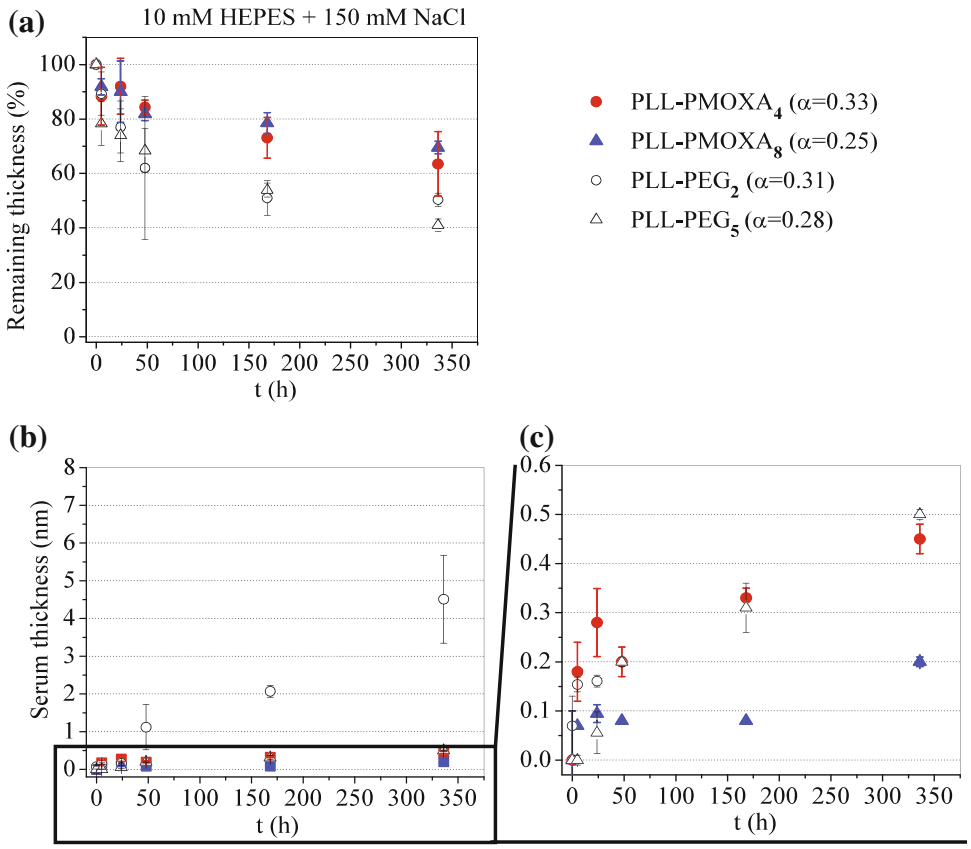

Fig. 4 **a** Remaining thickness of polymer films and **b**, **c** corresponding adsorbed serum thickness after stability tests in 10 mM HEPES + 150 mM NaCl

might be explained from slightly higher monomer surface density of PLL-PMOXA$_8$ compared to PLL-PMOXA$_4$.

XPS analysis performed on initial and degraded copolymer films provided additional information on the possible degradation mechanism of the polymer films studied. Comparative analysis of the remaining C/Nb intensities showed around 10–15% signal decrease from PLL-PMOXA films after 1 day, and around 20% after 1 week of stability test (Fig. 5a). Remaining N/Nb shows very similar values as remaining C/Nb. For PLL-PMOXA, C and N are characteristic for both PMOXA and PLL.

The same experimental conditions resulted in 10–20 and 40–50% C/Nb loss for PLL-PEG films after 1 day and 1 week, respectively (Fig. 5b). Only 5–10 and 15–25% N/Nb reduction (N is characteristic of PLL but not PEG) for the same duration indicates that the film degradation was not simply due to copolymer detachment, but that PEG chains degraded preferentially to PLL. In a control experiment, PLL film showed only ~5% decrease of N/Nb over 1 week, in the same stability test solution (data not shown).

Furthermore, the C1s signal from PLL-PEG films could be deconvoluted into three component peaks: C–**C**–C (aliphatic C) at 285.0 eV, C–**C**–O (overlaps with C–**C**–N) at 286.7 eV, and **C**=O at 288.6 eV (See Table 2). Among these peaks, C–**C**–C and **C**=O peaks are exclusively characteristic of the PLL backbone, while C–**C**–O peak which overlaps with C–**C**–N peak is characteristic to both PEG and PLL, with approximately 98% contribution from C–**C**–O characteristic to PEG chains. Thus, the remaining C–**C**–O/(**C**=O+C–**C**–C) ratio was used to determine the remaining chemical composition of PLL-PEG layers on the surface (Fig. 6).

In Fig. 6, both PLL-PEG$_2$ and PLL-PEG$_5$ showed ~20% decrease in the PEG/PLL ratio after 1 day of exposure to 10 mM HEPES + 150 mM NaCl, indicating PEG degradation preferentially to PLL. The PEG/PLL ratio further decreased over 1 week of stability test, resulting in a total of ~40% of PEG loss, relative to the initial value. This is in a close agreement with previously published result of Zoulalian et al. [35] where ~30% of PEG loss was observed upon stability test of PLL-PEG$_2$- modified Nb_2O_5 surfaces in the same solution for 1 week.

3.3.3 Stability upon Exposure to Physiological Solution in the Presence of Oxidative Substance (10 mM H_2O_2 + 10 mM HEPES + 150 mM NaCl, pH = 7.4)

In addition to the stability tests in 10 mM H_2O_2 and physiological solution (10 mM + 150 mM NaCl), a

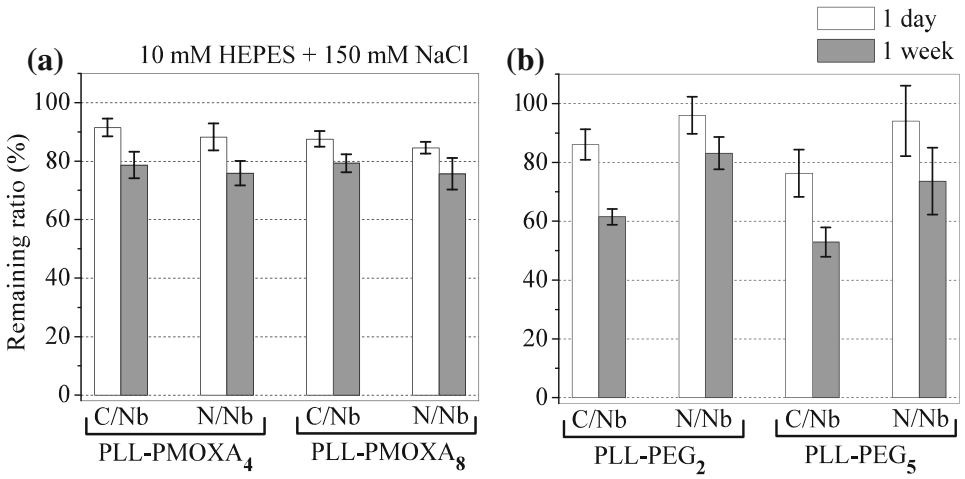

Fig. 5 Remaining C/Nb and N/Nb after 1 day and 1 week of stability tests in 10 mM HEPES + 150 mM NaCl for **a** PLL-PMOXA and **b** PLL-PEG films. Values were normalized to the initial values of the respective film

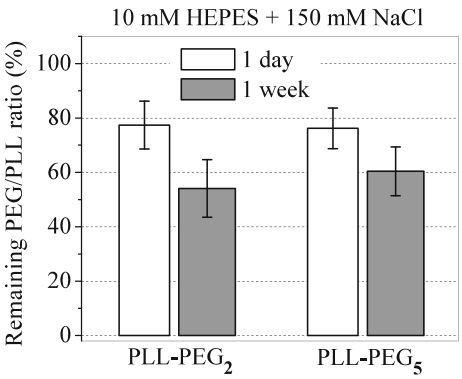

Fig. 6 Remaining PEG/PLL ratio of PLL-PEG films after 1 day and 1 week of stability test in 10 mM HEPES + 150 mM NaCl, as judged from C–**C**–O/(**C**=O+C–**C**–C) ratio. All values were normalized to the initial values of the respective film

stability study of PLL-PEG and PLL-PMOXA films in the mixture of 10 mM H_2O_2 and 10 mM HEPES + 150 mM NaCl was performed.

VASE was used for straightforward data comparison with the results obtained from two previous stability studies. An exposure time of 5 h was chosen in order to allow comparison with the results obtained by OWLS (see below). Figure 7 shows remaining film thickness for PLL-PEG, PLL-PMOXA, and PLL after incubation in the three chosen media.

While PLL-PMOXA films remained more stable (only 5–10% decrease), 40–45% decrease in thickness was observed for PLL-PEG films in the mixture of 10 mM H_2O_2 + 10 mM HEPES + 150 mM NaCl (Fig. 7). This value shows that the degradation of PLL-PEG films proceeded faster in this solution when compared to either H_2O_2 or 10 mM HEPES + 150 mM NaCl solution.

Complementary to the ex situ techniques, in situ OWLS analysis was applied to monitor the degradation kinetics over time. Considering the baseline drift issue in OWLS technique [52], time duration of 5 h was considered to be a good compromise. Exemplary OWLS spectra are presented in Fig. 8a, b for PLL-PMOXA$_4$ ($\alpha = 0.33$) and PLL-PEG$_2$ ($\alpha = 0.31$). Incubation of the Nb_2O_5-coated waveguides in copolymer solutions during 30–120 min (step 1) followed by rinsing with buffer solution (step 2) resulted in saturation of layers with the following adsorbed mass values (evaluated according to previously published protocol) [19, 20]: 210 ng/cm^2 (PLL-PMOXA$_4$) and 152 ng/cm^2 (PLL-PEG$_2$). Subsequent injection of 10 mM H_2O_2 in 10 mM HEPES + 150 mM NaCl buffer (step 3) followed by further 5 h incubation and rinsing with buffer solution (step 4) caused loss of the adsorbed copolymer mass up to 25 ng/cm^2 for PLL-PMOXA$_4$ and 90 ng/cm^2 for PLL-PEG$_2$. Addition of full serum to the degraded films (step 5) followed by rinsing with buffer solution (step 6) resulted in adsorbed serum protein mass values of 3 and 20 ng/cm^2 for PLL-PMOXA$_4$ and PLL-PEG$_2$ films, respectively. The experiments were repeated three times for each copolymer, and the averaged results with standard deviations are presented in Fig. 8c. The PLL-PMOXA$_4$ and PLL-PMOXA$_8$ film lost only 10 and 20% of the initial mass, respectively, whereas PLL-PEG$_2$ and PLL-PEG$_5$ films experienced much higher mass reduction by 60 and 40% of their initial values, respectively. These results confirmed that PLL-PMOXA films exhibited significantly better stability than PLL-PEG films under the applied experimental conditions and remained largely resistant to protein adsorption (3 ± 3 and 1 ± 1 ng/cm^2 of adsorbed serum for PLL-PMOXA$_4$ and PLL-PMOXA$_8$, respectively), in stark contrast to the PEG copolymers (21 ± 4 and 13 ± 4 ng/cm^2 of adsorbed serum for PLL-PEG$_2$ and PLL-PEG$_5$, respectively). A control stability experiment on a PLL film upon exposure to the same solution showed almost no reduction in adsorbed mass, confirming its high stability (data not shown).

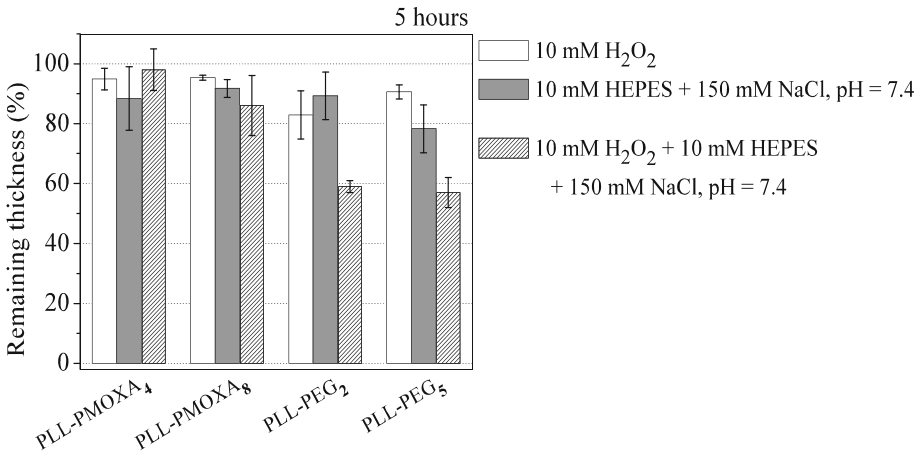

Fig. 7 Remaining thickness of the different polymer films after 5 h incubation in stability test solutions: 10 mM H_2O_2 in ultrapure water, 10 mM HEPES + 150 mM NaCl, and 10 mM H_2O_2 in 10 mM HEPES + 150 mM NaCl

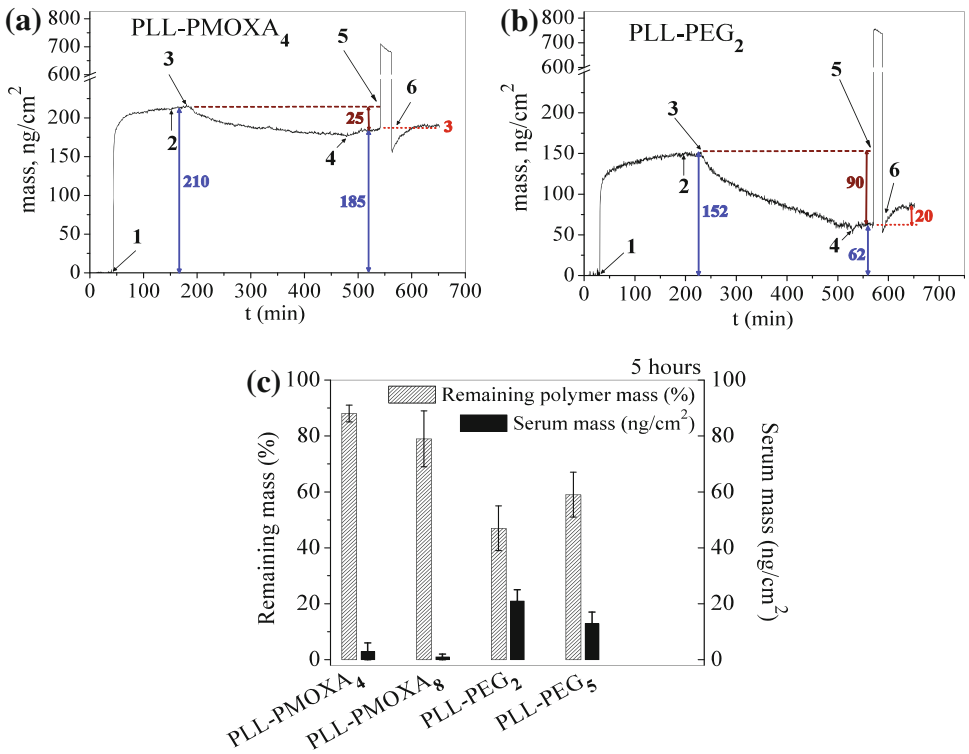

Fig. 8 Representative OWLS spectra: change of the adsorbed copolymer masses during initial polymer adsorption and stability tests under exposure to 10 mM H_2O_2 in 10 mM HEPES + 150 mM NaCl solution of: **a** PLL-PMOXA$_4$, **b** PLL-PEG$_2$. The stability study was followed by serum resistance test in case of PLL-PMOXA and PLL-PEG films. **c** Quantitative summary of the remaining copolymer masses and the corresponding adsorbed serum masses on the degraded films

3.3.4 Quantitative Correlation VASE, XPS, and OWLS Results, as well as between Copolymer Film Thickness and Serum Thickness and Mass

Figure 9a shows linear correlation between copolymer thickness measured by VASE (x-axis) and C/Nb ratio derived from XPS analysis (open symbols, left y-axis) as well as copolymer mass density measured by OWLS (solid symbols, right y-axis). At copolymer thickness of ~0 nm (bare Nb_2O_5), the corresponding C/Nb shows a non-zero value of ~0.22, which could be attributed to un-avoidable, adventitious carbon contamination. The linear correlation demonstrates that film thickness correlate quantitatively with both C/Nb and film mass density. Moreover, Fig. 9b shows that copolymer thickness correlates quantitatively with both serum thickness (open symbols, left y-axis) and serum mass density (solid symbols, right y-axis) on the copolymer film, i.e. serum thickness and serum mass decrease as copolymer thickness increases.

3.3.5 Hypotheses on the Degradation Mechanism of PLL-PEG and PLL-PMOXA Films

As shown and discussed above, incubation of copolymer films in the different stability test solutions lead to different levels of film degradation. Here we propose hypotheses on the degradation mechanisms.

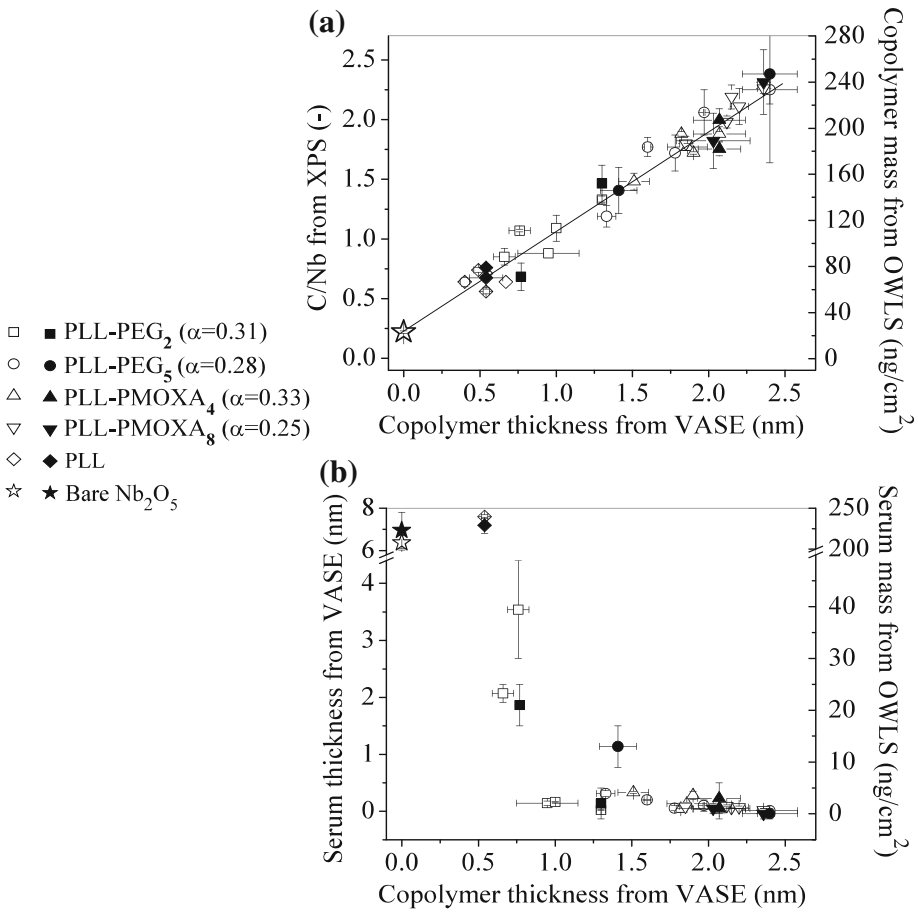

Fig. 9 **a** C/Nb from XPS (*open symbols*, left *y-axis*) and copolymer mass from OWLS (*solid symbols*, right *y-axis*) plotted against copolymer thickness from VASE (*x-axis*) and **b** serum thickness from VASE (*open symbols*, left *y-axis*) and serum mass from OWLS (*solid symbols*, right *y-axis*) on copolymer film plotted against copolymer thickness from VASE (*x-axis*)

10 mM H_2O_2 solution was used to simulate in vivo conditions [upon phagocytosis, macrophages produce superoxide (O_2^-) and hydrogen peroxide (H_2O_2)]. These reactive oxygen species can produce highly toxic radicals such as hydroxyl radicals (HO^*) which may directly promote the oxidative polymer degradation at the surface [48].

Degradation of copolymer films in 10 mM HEPES + 150 mM NaCl solution is less intuitive. HEPES has been reported to strongly take part in radical reactions [53–55]. Most importantly, under the influence of light, HEPES-containing cell culture solutions have been found to form hydrogen peroxide in a light-dose dependent manner. Furthermore, the piperazine ring as well as the alcohol function of HEPES can act as a hydroxyl radical scavenger and HEPES can form nitroxide-type radicals at the piperazine function. These findings suggest that HEPES might promote the oxidative degradation of polymers in biological media not protected from oxygen and light. In this study, all samples were protected from light by covering the containers with aluminum foil during the stability test period. However, solutions were not degassed and it is likely that reactive oxygen species were formed during the preparation of ultrapure water which involves UV light exposure to degrade organic contaminants. These reactive oxygen species might subsequently have reacted with HEPES. This could also explain the observed synergistic action of HEPES and hydrogen peroxide containing solutions on polymer degradation.

An alternative explanation for film instability would be the detachment of entire graft copolymer molecules from the Nb_2O_5 substrate. We have ruled out this mechanism by XPS measurements showing that the PEG signal decreases faster than the PLL signal during exposure to the stability test solutions. This shows that the graft copolymer side chains degrade while the backbone polymer, PLL, remains electrostatically bound to the substrate.

4 Summary and Conclusions

We found that the degradation rates differed significantly between PLL-PEG and PLL-PMOXA films, with the latter showing better stability in all model environments tested in this work. The higher stability of PLL-PMOXA films compared to PLL-PEG films was proven by surface analysis performed using three complementary techniques (VASE, XPS, and OWLS). Despite the similar architecture of the PMOXA- and PEG-copolymers used in terms of

grafting density, initial adsorbed mass (thickness), molecular-, side chain-, and monomer-surface density, as well as initial C/Nb ratio, films prepared from PLL-PMOXA always showed considerably higher stability when compared to PLL-PEG.

Although the film degradation mechanisms could not be fully deciphered, the XPS analysis supports the hypothesis that the stability of PLL-PMOXA and PLL-PEG films is primarily limited by the side chain (PMOXA or PEG) degradation. Further investigations are needed to gain a deeper understanding on the exact degradation mechanism as well as on the degradation products of PLL-PMOXA and PLL-PEG films.

In conclusion, this study suggests PMOXA coatings as a potent alternative to PEG coatings due to their higher stability in physiological and oxidative environments and related prolonged resistance to protein fouling. The findings of this work are believed to also be relevant in the context of application of polymeric, anti-fouling surfaces in vivo. Degradation of polymers that result in the production of reactive species such as radicals, hydrogen peroxide or hydrogen superoxide are likely to contribute to an inflammatory and foreign body response by the host resulting in encapsulation of the biomaterial or medical device by the formation of an avascular capsule. It would be interesting in our view to investigate whether PMOXA-modified biomaterial surfaces would result in a more natural healing and integration when implanted in (soft) tissue in comparison to PEG. Complementary investigations are underway.

Acknowledgments We acknowledge financial support from the Swiss National Science Foundation (SNSF, Project 200021-116163) and Materials for the Life Sciences Unit of the Swiss Competence Center for Materials Research and Technology of the ETH Domain.

References

1. Kenausis GL, Vörös J, Elbert DL, Huang N, Hofer R, Ruiz-Taylor L, Textor M, Hubbell JA, Spencer ND (2000) J Phys Chem B 104:3298
2. Maddikeri RR, Tosatti S, Schuler M, Chessari S, Textor M, Richards RG, Harris LG (2008) J Biomed Mater Res Part A 84A:425
3. Lussi JW, Falconnet D, Hubbell JA, Textor M, Csucs G (2006) Biomaterials 27:2534
4. Roosjen A, Norde W, van der Mei HC, Busscher HJ (2006) Program Colloid Polym Sci 132:138
5. Malmsten M, Emoto K, Van Alstine JM (1998) J Colloid Interface Sci 202:507
6. McPherson T, Kidane A, Szleifer I, Park K (1998) Langmuir 14:176
7. Sofia SJ, Premnath V, Merrill EW (1998) Macromolecules 31:5059
8. Dalsin JL, Lin L, Tosatti S, Vörös J, Textor M, Messersmith PB (2005) Langmuir 21:640
9. Pasche S, DePaul SM, Vörös J, Spencer ND, Textor M (2003) Langmuir 19:9216
10. Feller LM, Cerritelli S, Textor M, Hubbell JA, Tosatti SGP (2005) Macromolecules 38:10503
11. Roosjen A, Kaper HJ, van der Mei HC, Norde W, Busscher HJ (2003) Microbiology 149:3239
12. Koh WG, Revzin A, Simonian A, Reeves T, Pishko M (2003) Biomed Microdevices 5:11
13. Park JH, Bae YH (2003) J Appl Polym Sci 89:1505
14. Harris LG, Tosatti S, Wieland M, Textor M, Richards RG (2004) Biomaterials 25:4135
15. Marie R, Beech JP, Vörös J, Tegenfeldt JO, Hook F (2006) Langmuir 22:10103
16. Cringus-Fundeanu I, Luijten J, van der Mei HC, Busscher HJ, Schouten AJ (2007) Langmuir 23:5120
17. Abd El-Mohdy H, Ghanem S (2009) J Polym Res 16:1
18. Statz AR, Meagher RJ, Barron AE, Messersmith PB (2005) J Am Chem Soc 127:7972
19. Konradi R, Pidhatika B, Mühlebach A, Textor M (2008) Langmuir 24:613
20. Pidhatika B, Möller J, Vogel V, Konradi R (2008) CHIMIA Int J Chem 62:264
21. Pidhatika B, Möller J, Benetti EM, Konradi R, Rakhmatuliina E, Muehlebach A, Zimmermann R, Werner C, Vogel V, Textor M (2010) Biomaterials 31:9462
22. Veronese FM, Pasut G (2005) Drug Discov Today 10:1451
23. Pasut G, Veronese FM (2009) Adv Drug Deliv Rev 61:1177
24. Matthews SJ, McCoy C (2004) Clin Ther 26:991
25. Donbrow M (1987) In: Schick MJ (ed) Nonionic surfactants: physical chemistry, vol. 23. Marcel Dekker, New York
26. Shen M, Martinson L, Wagner MS, Castner DG, Ratner BD, Horbett TA (2002) J Biomater Sci Polym Ed 13:367
27. Roosjen A, Vries Jd, van der Mei HC, Norde W, Busscher HJ (2005) J Biomed Mater Res B Appl Biomater 73B:347
28. McGary-Jr CW (1960) J Polym Sci Part A Polym Chem 46:51
29. Han S, Kim C, Kwon D (1995) Polym Degrad Stab 47:203
30. Branch DW, Wheeler BC, Brewer GJ, Leckband DE (2001) Biomaterials 22:1035
31. Sharma S, Johnson RW, Desai TA (2003) Langmuir 20:348
32. Zhang F, Kang ET, Neoh KG, Wang P, Tan KL (2001) J Biomed Mater Res 56:324
33. Bindra DS, Williams TD, Stella VJ (1994) Pharm Res 11:1060
34. Knop K, Hoogenboom R, Fischer D, Schubert US (2010) Angew Chem Int Ed 49:6288
35. Zoulalian V, Zürcher S, Tosatti S, Textor M, Monge S, Robin JJ (2009) Langmuir 26:74
36. Imamura S-i, Tonomura Y, Kawabata N, Kitao T (1981) Bull Chem Soc Jpn 54:1548
37. Chilkoti A, Dreher MR, Meyer DE, Raucher D (2002) Adv Drug Deliv Rev 54:613
38. Yamaoka T, Tabata Y, Ikada Y (1994) J Pharm Sci 83:601
39. von Erlach T, Zwicker S, Pidhatika B, Konradi R, Textor M, Hall H, Lühmann T (2011) Biomaterials 32:5291
40. Woodle MC, Engbers CM, Zalipsky S (1994) Bioconjugate Chem 5:493
41. Hoogenboom R (2009) Angew Chem Int Ed 48:7978
42. Zalipsky S, Hansen CB, Oaks JM, Allen TM (1996) J Pharm Sci 85:133
43. Cheon Lee S, Kim C, Chan Kwon I, Chung H, Young Jeong S (2003) J Control Release 89:437

44. Broz P, Benito SM, Saw C, Burger P, Heider H, Pfisterer M, Marsch S, Meier W, Hunziker P (2005) J Control Release 102:475
45. Ranquin A, Versees W, Meier W, Steyaert J, Van Gelder P (2005) Nano Lett 5:2220
46. Zaikov GE (1985) Polym Rev (Philadelphia, PA, US) 25: 551
47. Williams DF (1982) J Mater Sci 17:1233
48. Ali SAM, Doherty PJ, Williams DF (1994) J Appl Polym Sci 51:1389
49. Statz AR, Kuang J, Ren C, Barron AE, Szleifer I, Messersmith PB (2009) Biointerphases 4: FA22
50. Tompkins HG, McGahan WA (1999) Spectroscopic ellipsometry and reflectometry: a user's guide. Wiley, New York
51. Moulder JF, Chastain J (1992) Handbook of X-ray photoelectron spectroscopy: a reference book of standard spectra for identification and interpretation of XPS data. Physical Electronics Division, Perkin-Elmer Corp., Eden Prairie
52. Vörös J, Ramsden JJ, Csúcs G, Szendro I, De Paul SM, Textor M, Spencer ND (2002) Biomaterials 23:3699
53. Zigler J, Lepe-Zuniga J, Vistica B, Gery I (1985) In Vitro Cell Develop Biol Plant 21:282
54. Lepe-Zuniga JL, Zigler JS Jr, Gery I (1987) J Immunol Methods 103:145
55. Grady JK, Chasteen ND, Harris DC (1988) Anal Biochem 173:111